Observation of femtojoule optical bistability involving Fano resonances in high-Q/V_m silicon photonic crystal nanocavities

Xiaodong Yang,[a] Chad Husko, and Chee Wei Wong[b]
Optical Nanostructures Laboratory, Columbia University, New York, New York 10027

Mingbin Yu and Dim-Lee Kwong
The Institute of Microelectronics, 11 Science Park Road, Singapore 117685, Singapore

(Received 12 March 2007; accepted 21 June 2007; published online 31 July 2007)

The authors observe experimentally optical bistability enhanced through Fano interferences in high-Q localized silicon photonic crystal resonances ($Q\sim 30\,000$ and modal volume ~ 0.98 cubic wavelengths). This phenomenon is analyzed through nonlinear coupled-mode formalism, including the interplay of $\chi^{(3)}$ effects such as two-photon absorption and related free-carrier dynamics, and optical Kerr as well as thermal effects and linear losses. Experimental and theoretical results demonstrate Fano resonance based bistable states with switching thresholds of 185 μW and 4.5 fJ internally stored cavity energy ($\sim$540 fJ consumed energy) in silicon for scalable optical buffering and logic. © *2007 American Institute of Physics*. [DOI: 10.1063/1.2757607]

Two-dimensional photonic crystal nanocavities with remarkable high quality factors (Q) and subwavelength modal volumes (V_m) at $\sim(\lambda/n)^3$ (Refs. 1 and 2) have been achieved recently. The strong localization and long photon lifetimes in these high-Q/V_m photonic crystal nanocavities point to enhanced nonlinear optical physics, such as Lorentzian-cavity-based bistability,[3–7] Raman lasing,[8,9] and cavity QED (Ref. 10) in silicon photonics.

The interference of a discrete energy state with a continuum can give rise to sharp and asymmetric line shapes, referred to Fano resonances.[11,12] Compared to a Lorentzian resonance, these line shapes arise from temporal pathways that involve direct and indirect (for example, a resonance) transmissions, with a reduced frequency shift required for nonlinear switching due to its sharper line shape. If the indirect pathway can be further strongly localized (such as in a high-Q/V_m cavity), the nonlinear characteristic switching thresholds can be further reduced. Optical bistability involving Fano resonances due to Kerr effect in photonic crystal cavities has been theoretically studied based on Green's function solution of Maxwell's equations.[13] Fano resonances have also been studied by transfer matrix technique,[12,14] and coupled-mode equations.[15]

In this letter, we present our measurements on Fano-based optical bistability as well as a temporal nonlinear coupled-mode framework for numerical analysis. Figure 1(a) shows a schematic of the theoretical model. A waveguide with two partially reflecting elements is side coupled to a cavity. a is the amplitude of the cavity mode to represent the energy $U=|a|^2$ and s is the amplitude of the waveguide mode to represent the power $P=|s|^2$. With the coupled-mode formalism,[16,17] the dynamic equation for $a(t)$ is[15,18]

$$\frac{da}{dt}=\left(-\frac{1}{2\tau_{\text{total}}}+i(\omega_0+\Delta\omega-\omega_{\text{wg}})\right)a+\kappa s_{a1+}+\kappa s_{a2+}. \tag{1}$$

As shown in Fig. 1(a), $s_{a1-}=\exp(-i\phi)s_{a2+}+\kappa a$ and $s_{a2-}=\exp(-i\phi)s_{a1+}+\kappa a\cdot\phi=\omega_{\text{wg}}n_{\text{eff}}L/c$ is the phase shift. κ is the coupling coefficient between $s(t)$ and $a(t)$, and $\kappa=i\exp(-i\phi/2)/\sqrt{2\tau_{\text{in}}}$.[18] For a lossy partially reflecting element with the amplitude reflectivity r and transmissivity t ($r^2+t^2\leq 1$) (Ref. 16),

$$\begin{pmatrix}s_{aj+}\\ s_{aj-}\end{pmatrix}=\frac{1}{it}\begin{pmatrix}-(r^2+t^2) & -r\\ r & 1\end{pmatrix}\begin{pmatrix}s_{j+}\\ s_{j-}\end{pmatrix},\quad j=1,2. \tag{2}$$

In Eq. (1), the total loss rate $1/\tau_{\text{total}}$ includes the effects of radiation, linear material absorption, two-photon absorption (TPA), and free-carrier absorption.[3,5,8] The $\Delta\omega$ detuning of the cavity resonance from ω_0 is modeled due to the Kerr effect, free-carrier dispersion, and thermal dispersion effects under first-order perturbation. With the modeled TPA generated carrier dynamics and thermal transients [Eqs. (31) and (42) in Ref. 8], the coupled nonlinear dynamical behavior of the Fano optical system is numerically integrated.

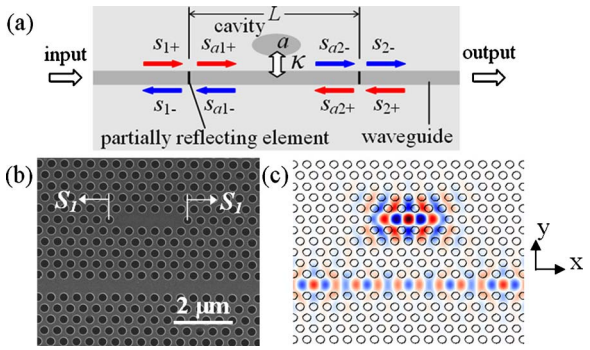

FIG. 1. (Color online) (a) Schematic of optical system including a waveguide side coupled to a cavity. Two partially reflecting elements are placed in the waveguide. (b) Scanning electron microscopy of photonic crystal $L5$ point-defect cavity side coupled to line-defect waveguide. (c) E_y field of the resonance mode midslab from 3D FDTD simulations.

[a]Electronic mail: xy2103@columbia.edu
[b]Electronic mail: cww2104@columbia.edu

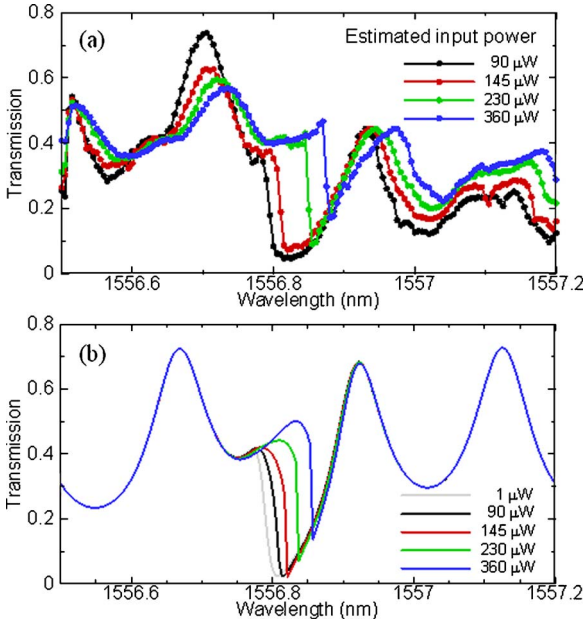

FIG. 2. (Color online) (a) Measured and (b) coupled-mode theory (CMT)-calculated transmission spectrum at different input powers.

The optical system consisting of a photonic crystal waveguide side coupled to a high-Q/V_m $L5$ nanocavity in an air-bridge triangular lattice photonic crystal slab with thickness of $0.6a$ and the radius of air holes is $0.29a$, where the lattice period $a=420$ nm, as shown in Fig. 1(b). The shift S_1 of two air holes is $0.02a$ to tune the radiation mode pattern for increasing the Q factors. The index contrast at the waveguide input and output facets acts as a partially reflecting element with distance L of around 1.9 mm to form a Fabry-Pérot resonator and perturb the phase of the waveguide mode.

The devices were fabricated with the standard integrated circuit techniques in a silicon-on-insulator substrate. A polarization controller and a lensed fiber are used to couple transverse-electric polarization light from tunable laser source into the waveguide. A second lensed fiber collects the transmission from the waveguide output that is sent to the photodetector and lock-in amplifier. The input power coupled to the waveguide is estimated from the total transmission loss of the whole system,[5] which is around 24.8 dB at 1555 nm. At low input power of 20 μW, the measured resonant wavelength λ_0 is 1556.805 nm. To measure the Q factor, the vertical radiation from the top of only $L5$ nanocavity is collected. The estimated Q, based on the full width at half maximum $\Delta\lambda$ of 52 pm, is ~30 000. From three-dimensional (3D) finite-difference time-domain (FDTD) method, the total Q is ~31 000.

Figure 2(a) shows the measured transmission spectrum with different input powers. Sharp and asymmetric Fano line shapes are observed. The spectral line shapes depend on the position of cavity resonance in a Fabry-Pérot background, highlighting Fano interference pathways. Here the spectra show ascending Fano resonances. The Fabry-Pérot fringe spacing $d\lambda$ is around 230 pm, which corresponds to the distance between two waveguide facets $d=1.902$ mm [$d=\lambda^2/(2d\lambda n_{\text{eff}})$ and effective index of 2.77 from FDTD simulations]. As the input power increases, the Fano line shapes were redshifted due to TPA induced thermo-optic nonlinearities in silicon.[3–5] Figure 2(b) shows the calculated transmission spectrum from nonlinear coupled-mode model. All parameters are from either reference papers or FDTD results.[8] When the input power is 1 μW or less, the cavity response is in the linear regime. As the input power increases, the Fano line shapes were redshifted.

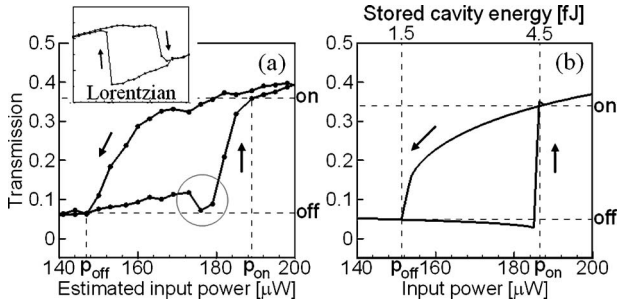

FIG. 3. (a) Measured and (b) CMT-calculated asymmetric hysteresis loops for Fano resonance at a detuning of 22 pm. The inset of (a) shows the measured hysteresis loop for Lorentzian resonance.

Figure 3(a) shows the observed hysteresis loop of Fano resonance at red detuning δ of 22 pm ($\delta/\Delta\lambda=0.423$). For comparison, the inset of Fig. 3(a) shows the measured hysteresis loop for Lorentzian resonance. The bistable loops of ascending Fano line shapes are very distinct from Lorentzian line shapes. Firstly, one suggestive indication is the asymmetry in the hysteresis loop, with sharp increase (gentle decrease) with increasing (decreasing) power for lower (upper) branch, resulting from the asymmetric Fano line shape. Secondly, for ascending Fano resonances, an important indication is the upward slope (*increase* in transmission) for increasing input power for a side-coupled cavity. For a symmetric Lorentzian in a side-coupled cavity, a downward slope (or decrease in transmission) should be expected for increasing input power.[19–21] Thirdly, the dip in the transmission [as indicted by the dotted red circle in Fig. 3(a)] is another signature of the Fano resonance. This feature is not observable with a symmetric Lorentzian and in fact is an aggregate result of the three self-consistent solutions of the nonlinear Fano system, such as predicted using Green's function method in Ref. 13. Our nonlinear coupled-mode theory framework cannot trace out the individual solutions[13] but show the aggregate behavior and is in remarkable agreement with our experimental measurements and the Green's function predictions.

The Fano bistable "off" power (p_{off}) is estimated at 147 μW and the "on" power (p_{on}) at 189 μW for a 22 pm detuning, as shown in Fig. 3(a). From the 189 μW (147 μW) p_{on} (p_{off}) thresholds, this corresponds to an estimated internally stored cavity energy[3] of 4.5 fJ (1.5 fJ) based on a numerical estimate of waveguide-to-cavity coupling coefficient (κ^2) of 13.3 GHz. The consumed energy, in terms of definition used in Ref. 20, is ~540 fJ (60 fJ) based on the numerical estimated thermal relaxation time of 25 ns and 11.4% (1.6%) of input power absorbed by TPA process for on (off) state, although this could be much lower with minimum detuning to observe bistability. The femtojoule level switching in the stored cavity energy is due to the lowered threshold from the sharp Fano interference line shape, the small mode volume and high-Q photonic crystal cavities. For the 22 pm detuning, the switching intensity contrast ratio is estimated at 8.5 dB with a $p_{\text{on}}/p_{\text{off}}$ ratio of 1.286. Figure 3(b) shows the calculated Fano bistable hysteresis at

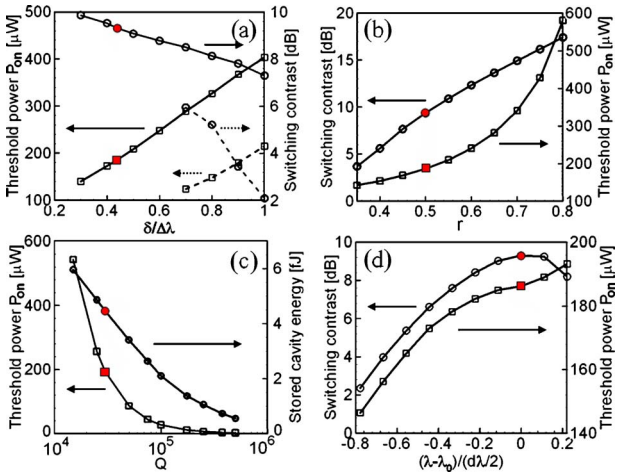

FIG. 4. (Color online) (a) CMT-calculated effects of the wavelength detuning $\delta/\Delta\lambda$. Dashed lines (--) represent Lorentzian bistability which, compared to this particular Fano-type bistability, requires higher detuning to observe bistability and results in lower switching contrast. Effects of (b) mirror reflectivity r, (c) cavity Q factor, and (d) the position of cavity resonance on the switching threshold power p_{on} and switching contrast. (The red-filled symbols correspond to the experimental parameters.)

the detuning of 22 pm from nonlinear coupled-mode theory. The calculated p_{off} and p_{on} thresholds are 151 μW (with the stored cavity energy of 1.5 fJ) and 186 μW (4.5 fJ) respectively, with a switching contrast of 9.3 dB and p_{on}/p_{off} ratio of 1.232, in excellent agreement with the experimental results.

Now we examine parametrically the dependence of the Fano-type bistability against achievable device characteristics, with our developed nonlinear model. Figure 4 summarizes the extensive numerically calculated effects of normalized detuning ($\delta/\Delta\lambda$), mirror reflectivity r, cavity Q, the position of cavity resonance on the characteristic threshold power p_{on}, and switching contrast. A base line Q of 30 000, a r of 0.5 with 11% mirror loss, a λ_0 of 1556.805 nm, and a detuning $\delta/\Delta\lambda$ of 0.423 are used, which correspond to the current experimental parameters and are represented as the red-filled symbols in Fig. 4. In Fig. 4(a), the minimum detuning required for Lorentzian bistability ($r=0$, dashed lines) is $\delta/\Delta\lambda \sim 0.7$, which agrees well with the theoretical threshold detuning $\delta/\Delta\lambda = \sqrt{3}/2$.[22] However, the threshold detuning for Fano bistability (solid lines) to appear is $\delta/\Delta\lambda \sim 0.3$, which is much smaller than Lorentzian case. The threshold power is similar for both cases (around 140 μW) at the threshold detuning. Compared to Lorentzian bistability, Fano bistability has higher switching contrast and it decreases more slowly with increased wavelength detuning. The low threshold detuning and high switching contrast for Fano bistability is due to the sharp and asymmetric Fano line shapes. This switching contrast can significantly increase when the mirror reflectivity r increases from 0.35 to 0.8 at the expense of increasing p_{on} [Fig. 4(b)]. For cavity Q factor of half a million, the Fano threshold power is estimated at 2.4 μW, which corresponds to the stored cavity energy of 0.55 fJ [Fig. 4(c)]. Figure 4(d) illustrates the influence of different positions of cavity resonance λ relative to experimental λ_0 within the half period of Fabry-Pérot background $d\lambda/2$, where the limits of $(\lambda-\lambda_0)/(d\lambda/2)$ are from −0.8 to 0.2 for ascending Fano resonances. Both threshold power and switching contrast increase as the cavity resonance λ shifts from the Fabry-Pérot background maximum to its minimum. The Fano resonance has little control in the current configuration, either ascending or descending Fano resonance can be obtained, depending on the position of cavity resonance in the Fabry-Pérot background formed by two waveguide facets. In the future, integrated partially reflecting mirrors embedded inside photonic crystal waveguide can be adopted to tune the Fabry-Pérot background for the designed Fano line shapes.[23]

In this work we demonstrate experimentally all-optical bistability arising from sharp Fano resonances in high-Q/V_m silicon photonic crystal nanocavities. Using the TPA induced thermo-optic nonlinearity, on-state threshold of 189 μW and stored cavity energy of 4.5 fJ are observed and in good agreement with the nonlinear coupled-mode formalism. Our observations of Fano-type bistability highlight the feasibility of an ultralow energy and high contrast switching mechanism in monolithic silicon benefiting from the sharp Fano line shapes, for scalable functionalities, such as all-optical switching, memory, and logic for information processing.

This work was partially supported by DARPA and the National Science Foundation (ECCS-0622069). One of the authors (X.Y.) acknowledges the support of an Intel Fellowship.

[1] B. S. Song, S. Noda, T. Asano, and Y. Akahane, Nat. Mater. **4**, 207 (2005).
[2] E. Kuramochi, M. Notomi, S. Mitsugi, A. Shinya, T. Tanabe, and T. Watanabe, Appl. Phys. Lett. **88**, 041112 (2006).
[3] P. E. Barclay, K. Srinivasan, and O. Painter, Opt. Express **13**, 801 (2005).
[4] T. Tanabe, M. Notomi, S. Mitsugi, A. Shinya, and E. Kuramochi, Appl. Phys. Lett. **87**, 151112 (2005).
[5] T. Uesugi, B. Song, T. Asano, and S. Noda, Opt. Express **14**, 377 (2006).
[6] V. R. Almeida, C. A. Barrios, R. R. Panepucci, and M. Lipson, Nature (London) **431**, 1081 (2004).
[7] E. Weidner, S. Combrié, A. de Rossi, N.-V.-Q. Tran, and S. Cassette, Appl. Phys. Lett. **90**, 10118 (2007).
[8] X. Yang and C. W. Wong, Opt. Express **15**, 4763 (2007).
[9] H. Rong, R. Jones, A. Liu, O. Cohen, D. Hak, A. Fang, and M. Paniccia, Nature (London) **433**, 725 (2005).
[10] R. Bose, X. Yang, R. Chatterjee, J. Gao, and C. W. Wong, Appl. Phys. Lett. **90**, 111117 (2007).
[11] U. Fano, Phys. Rev. **124**, 1866 (1961).
[12] S. Fan, Appl. Phys. Lett. **80**, 908 (2002).
[13] A. R. Cowan and J. F. Young, Phys. Rev. E **68**, 046606 (2003).
[14] V. Lousse and J. P. Vigneron, Phys. Rev. B **69**, 155106 (2004).
[15] S. Fan, W. Suh, and J. D. Joannopoulos, J. Opt. Soc. Am. A **20**, 569 (2003).
[16] H. A. Haus, *Waves and Fields in Optoelectronics* (Prentice-Hall, Englewood Cliffs, NJ, 1984), Chap. 7, p. 197,
[17] A. Yariv, *Optical Electronics* (Sanders College, Philadelphia, PA, 1991), Chap. 13, 519.
[18] B. Maes, P. Bienstman, and R. Baets, J. Opt. Soc. Am. B **22**, 1778 (2005).
[19] M. F. Yanik, S. Fan, and M. Soljačić, Appl. Phys. Lett. **83**, 2739 (2003).
[20] M. Notomi, A. Shinya, S. Mitsugi, G. Kira, E. Kuramochi, and T. Tanabe, Opt. Express **13**, 2678 (2005).
[21] M.-K. Kim, I.-K. Hwang, S.-H. Kim, H.-J. Chang, and Y.-H. Lee, Appl. Phys. Lett. **90**, 161118 (2007).
[22] M. Soljačić, M. Ibanescu, S. G. Johnson, Y. Fink, and J. D. Joannopoulos, Phys. Rev. E **66**, 055601 (2002).
[23] X. Yang, C. Husko, and C. W. Wong, CLEO/QELS, Baltimore, Maryland, May 2007, Paper No. JThD119.